DOI: 10.1002/ejic.200800721

Synthesis, Characterisation and Optical Properties of Silica Nanoparticles Coated with Anthracene Fluorophore and Thiourea Hydrogen-Bonding Subunits

Pilar Calero,[a] Ramón Martínez-Máñez,*[a] Félix Sancenón,*[a] and Juan Soto[a]

Keywords: Silica nanoparticles / Molecular recognition / Anions / Fluorescence / Langmuir isotherm

Bifunctionalised hybrid silica nanoparticles have been synthesised and characterised, and their optical emission properties in the presence of certain anions in acetonitrile solutions have been studied. The alkoxysilane derivatives *N*-butyl-*N*′-[3-(trimethoxysilyl)propyl]thiourea (**1**), *N*-phenyl-*N*′-[3-(trimethoxysilyl)propyl]thiourea (**2**) and 3-[(anthracen-10-yl)methylthio]propyltriethoxysilane (**3**) were prepared and used to functionalise uncoated LUDOX silica nanoparticles with a mean diameter of 18 ± 2 nm. The functionalisation of the nanoparticle surfaces was carried out by two different approaches. The first approach relies on the consecutive grafting of the two subunits. In this protocol, the nanoparticles were first functionalised with anthracene derivative **3** (solid **NA**), and then treated with the corresponding binding sites **1** or **2** to result in the **NA-Pt$_3$** and **NA-Bt$_3$** solids. The second approach deals with the simultaneous grafting of **1** or **2** and the signalling subunit **3** in different ratios. This method was used for the preparation of the **NA$_1$Pt$_1$**, **NA$_1$Bt$_1$**, **NA$_1$Pt$_3$** and **NA$_1$Bt$_3$** nanoparticles. The bifunctionalised silica nanoparticles were characterised by using standard techniques. Acetonitrile suspensions of **NA** nanoparticles (5 mg in 20 mL) showed anthracene bands centred at ca. 350, 370 and 390 nm. Upon excitation at 365 nm, a typical emission band with fine structure in the 390–450 nm range was observed. Similar absorption and emission spectra were found for the bifunctionalised nanoparticles. The work is completed with a prospective study of the fluorescence of the prepared nanoparticles in the presence of organic (acetate, benzoate) and inorganic (F^-, Cl^-, Br^-, CN^-, HSO_4^- and $H_2PO_4^-$) anions. The apparent binding constants (adsorption constants) for the interaction of **NA-Pt$_3$** with anions in acetonitrile were determined by performing a Langmuir-type analysis of fluorescence titration data.

Introduction

There is an increasing interest in the development of new sensing methods and protocols for target guests, and a number of recent advances have been described in this area. In a classical design approach, chemosensors are built up by the combination of two groups, i.e. the binding site and the signalling unit, connected through covalent bonds. The binding site is usually designed or selected bearing in mind the size, shape and nature of the chemical species to be coordinated and ideally results in selective interactions with certain target guests. On the other hand, the signalling unit transforms the host–guest interaction into suitable chromofluorogenic changes[1] or redox potential shifts.[2] Usually only one type of signalling unit is used in chemosensing, although a few examples are known where chemosensors contain more than one type of signalling subunit.[3]

Among different chemosensing systems, those relying on transformations of the emission fluorescence behaviour are especially appealing. By following this approach, an amazing quantity of fluorescent chemosensors for the detection of metal cations,[4] organic and inorganic anions[5] and neutral species[6] have been synthesised and tested. In spite of these examples, many fluorescent chemosensors show several limitations such as lack of selectivity. Recently, as an alternative to the development of classical fluorogenic probes, self-assembled structures on surfaces have attracted increasing attention in chemistry.[7] Many of these systems involve the use of a number of relatively simple chemical units which are attached to the surface of nanoparticles or nanostructured solids. As a result of the molecular organisation into a solid support, novel functional properties have been reported in hybrid materials, which show enhanced application potential.[8] Additionally, from a supramolecular viewpoint, the functionalisation of nanostructured solids with certain groups to enhance recognition or switching effects is particularly appealing.[9] Thus, the functionalisation of inorganic supports with receptors and fluorescent dyes can overcome synthetic problems which arise when following the classical "binding site–signalling unit" approach

[a] Instituto de Química Molecular Aplicada (IQMA), Departamento de Química, Universidad Politécnica de Valencia, Camino de Vera s/n, 46022 Valencia Spain
Fax: +34-96-387-9349
E-mail: rmaez@qim.upv.es
fsanceno@upvnet.upv.es

and provide an efficient strategy for the preparation of fluorogenic sensing systems.

The organisation of photoactive molecules and coordinating units onto the surface of nanoparticles is still a relatively recent field that could lead to the design of novel hybrid materials for use as labels and/or sensors.[10] Besides the reported examples of dye adsorption onto nanoparticle surfaces, covalent grafting is necessary in order to obtain stable arrangements and avoid structural reorganisations due to either redistribution of the adsorbed dye on the surface or between the surface and the solution.[11] In addition, silica nanoparticles can be synthesised easily, and their surface can be modified by the use of well-known alkoxysilane chemistry.[12] This versatility makes silica nanoparticles a good choice as scaffoldings for the grafting of dyes and coordinating units, especially when considering that these materials are transparent to visible light and inert as far as energy- and electron-transfer processes are concerned. This approach also induces the generation of amplification and cooperative effects associated with the independent anchoring of binding sites and fluorophores in close proximity to the surface support.[13] For instance, this close arrangement allows intercommunication between both subunits without the need of a direct covalent link between them. Also, the grafting of the receptor and the fluorophores onto the nanoparticle surface can induce cooperative processes such as enhanced binding constants.[14]

This strategy has been successfully employed in the development of fluorescent silica nanoparticles for the recognition of certain metal cations. Tecilla, Tonellato and coworkers prepared silica nanoparticles functionalised with trialkoxysilane derivatives of picolinamides as receptors and dansylamides as fluorescent reporters for the fluorescent sensing of Cu^{2+}.[15] The picolinamide ligand complexes the Cu^{2+} ion, and the bound ion quenches the dansyl emission substantially in dmso. In further studies the same authors used a combinatorial approach to functionalise silica nanoparticles with other ligands and fluorophores in various ratios.[16] The cooperative and collective effects are achieved by the organisation of the components on the particle surface to form multivalent binding sites with an increased affinity for Cu^{2+} ions. The binding of a single metal cation leads to the quenching of up to ten fluorescent groups that are surrounding a receptor unit with the corresponding signal amplification. The same authors, in a recent work, prepared fluorescent silica nanoparticles coated with a 6-methoxy-8-(*p*-toluenesulfonamido)quinoline derivative that showed a selective emission enhancement in the presence of Zn^{2+} cations in ethanol/water (1:1, v/v) mixtures.[17]

Also, improved signalling by the independent preorganisation of receptors and signalling units has been observed for extended surfaces and self-assembled monolayers (SAMs). SAMs on glass are examples of difunctionalised surfaces where directional preorganisation facilitates communications between the binding group and the signalling subunits. One of the first examples was described by Crego-Calama et al.[18] In a first step a monolayer of {3-[(2-aminoethyl)amino]propyl}trimethoxysilane was formed on a glass substrate and then treated with dansyl chloride and succinimidyl 7-(dimethylamino)coumarin-4-acetate in order to attach two distinct fluorophores. Then the residual amino groups were converted into amide and urea groups that would act as binding sites. The addition of certain metal cations (Pb^{2+}, Cd^{2+} and Zn^{2+}) to the prepared hybrid materials induced several degrees of quenching of the appended fluorophore. The best results were obtained for Pb^{2+}. In a further evolution the same research group prepared chemosensor materials for both cations and anions by using a combinatorial approach where glass monolayers were functionalised with fluorescent groups (rhodamine derivatives) and coordinating units (amino, arylurea, alkylurea, arylamide, alkylamide, sulfonamide, urea and thiourea).[19]

Thus, the use of silica supports, as nanoparticles or locally "flat" surfaces, has led to new organic–inorganic hybrid materials with enhanced recognition features. However, as far as we know, only one example dealing with hybrid materials using silica nanoparticles for anion sensing has been described. This hybrid system is based on the bifunctionalisation of silica nanoparticle surfaces with a spiropyran photochrome as chromogenic reporter and a thiourea derivative as binding site.[20] The merocyanine form is selectively transformed into the corresponding spirocyclic structure in the presence of long-chain carboxylates because of a change in the polarity on the nanoparticle surface.

Bearing these facts in mind, we report herein the synthesis of novel hybrid materials based on silica nanoparticles functionalised with two subunits: a binding site (thiourea-based receptor) and a signalling fluorescent subunit (anthracene). The synthesis, characterisation and studies on the emission behaviour of suspensions of the prepared nanoparticles in the presence of certain organic and inorganic anions have been carried out.

Results and Discussion

Design, Synthesis and Characterisation

The binding sites and the signalling subunit used for the preparation of the hybrid nanoparticles are shown in Scheme 1. Binding molecules **1** and **2** were prepared by the reaction between (3-aminopropyl)trimethoxysilane and butyl isothiocyanate (for **1**) and phenyl isothiocyanate (for **2**) in dichloromethane in the presence of catalytic amounts of triethylamine. The final products were isolated in nearly quantitative yields by evaporation of dichloromethane and characterised by standard techniques. The ^{1}H NMR spectrum of compound **1** shows the signals of the N–H thiourea protons at δ = 6.20 and 6.37 ppm. The most important feature of the ^{1}H NMR spectrum of compound **2** was the apparition of the aromatic signals in the δ = 7.05–7.20 nm range and the signals of the N–H protons of the thiourea moiety centred at δ = 6.27 and 8.41 ppm. The downfield shift observed for the signals of the thiourea protons in receptor **2** relative to receptor **1** is related to the presence of the aromatic ring in the structure of the former. The formation of the thiourea moieties in **1** and **2** was also confirmed

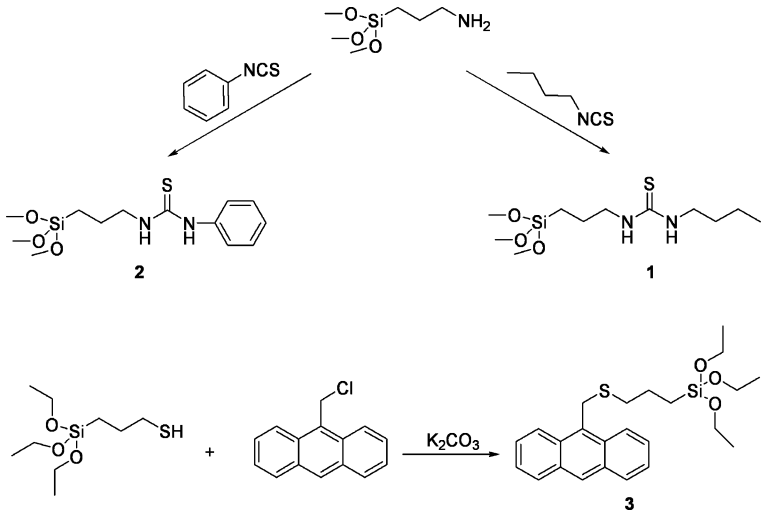

Scheme 1. Synthesis and structure of trialkoxysilane derivatives **1**–**3**.

by the presence of the thiourea quaternary carbon signal centred at δ = 181 ppm in the ^{13}C NMR spectrum.

The synthesis of anthracene derivative **3** was achieved by a nucleophilic substitution reaction between (3-mercaptopropyl)triethoxysilane and 9-(chloromethyl)anthracene in dry acetonitrile and potassium carbonate in a nearly quantitative yield. The ^{1}H NMR spectrum of compound **3** displays the typical signals of the anthracene moiety, i.e. two triplets centred at δ = 7.45 and 7.55 ppm, two pairs of doublets at δ = 8.00 and 8.33 ppm and a singlet centred at δ = 8.40 ppm. The spectrum is completed with a singlet at δ = 4.73 ppm assigned to the methylene group located between the anthracene unit and the sulfur atoms and two triplets at δ = 2.70 and 0.78 ppm assigned to the methylene moieties between the sulfur and silicon atoms.

Silica nanoparticles were selected as inorganic scaffoldings for the grafting of anion binding sites and signalling subunits due to their locally flat surfaces, known functionalisation reactions and easy dispersion in organic solvents. Coated silica nanoparticles were prepared by using the trialkoxysilyl derivatives **1**–**3** applying reported procedures by Montalti and co-workers.[21] In this synthetic protocol, commercially available silica nanoparticles were heated at 70 °C in a mixture of water/ethanol/acetic acid (1:2:1) in the presence of the coating subunits. Subsequent purification involved the evaporation of the ethanol, neutralisation of the acetic acid with sodium hydrogencarbonate, centrifugation and washings of the nanoparticles with acetone.

The functionalisation of the nanoparticle surface was carried out by two different approaches. The first approach relies on the consecutive grafting of the two subunits. In this protocol, the nanoparticles are first functionalised with anthracene moieties (solid **NA**) and then treated with the corresponding binding sites **1** or **2** to result in the **NA-Bt$_3$** and **NA-Pt$_3$** solids (the dash in this nomenclature indicates the two-step grafting process). The second approach deals with the simultaneous grafting of **1** or **2** and the signalling subunit **3** in different ratios. Different nanoparticles were simply prepared by modulation of the concentration of the alkoxysilane derivatives in the reaction mixture. This approach resulted in the preparation of nanoparticles identified as **NA$_x$Bt$_y$** and **NA$_x$Pt$_y$**, where the absence of the dash between the signalling and binding subunits indicates the simultaneous grafting process and the values of x and y specify the signalling/binding subunits molar ratios used in the reaction mixture. The **NA$_1$Bt$_1$**, **NA$_1$Pt$_1$**, **NA$_1$Bt$_3$** and **NA$_1$Pt$_3$** nanoparticles were prepared according to this procedure. A schematic representation of the hybrid fluorescent nanoparticles is shown in Figure 1. The amounts of binding sites and signalling subunits finally anchored on the different materials were determined through thermogravimetic analysis and SEM microanalysis (see Table 1).

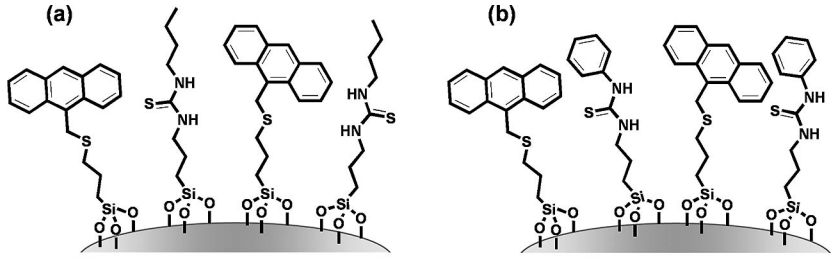

Figure 1. Schematic representation of the hybrid nanoparticules coated with butylthiourea and anthracene (a) and with phenylthiourea and anthracene (b).

Table 1. Contents of signalling subunit and binding site in hybrid nanoparticles.

	1 [mol/mol SiO_2]	2 [mol/mol SiO_2]	3 [mol/mol SiO_2]	Distance [Å]
NA	–	–	0.0042	22.1
NA-Pt$_3$	–	0.0125	0.0042	11.7
NA-Bt$_3$	0.0100	–	0.0042	12.8
NA$_1$Pt$_1$	–	0.0086	0.0086	11.6
NA$_1$Bt$_1$	0.0130	–	0.0130	9.4
NA$_1$Pt$_3$	–	0.0052	0.0017	19.0
NA$_1$Bt$_3$	0.0078	–	0.0026	14.8

As stated above, two different synthetic routes for the preparation of the bifunctionalised silica nanoparticles were studied. In the two-step grafting procedure, the anthracene-functionalised solid **NA** was first synthesised. A solid with a final content of 0.0042 mol **3**/mol SiO_2 was obtained. Transmission electron microscopy (TEM) measurements were carried out in order to determine the size and aggregation of the **NA** nanoparticles. Uncoated LUDOX silica nanoparticles showed a mean diameter of 18 ± 2 nm that changed to 20 ± 2 nm when they were grafted with **3** (solid **NA**). This significant increase in the mean diameter was attributed to the coating of the nanoparticle surfaces with the anthracene moiety. The number of anthracene moieties present on a single nanoparticle can be roughly estimated on the basis of three parameters: the anthracene content (determined by thermogravimetry and SEM microanalysis), the particle radii and the surface of the LUDOX nanoparticles. Through the approximation of a single monolayer of subunits on a smooth sphere, an average distance between two anthracenes of about 22.1 Å was determined.[22]

For the preparation of the **NA-Pt$_3$** and **NA-Bt$_3$** solids, the **NA** nanoparticles were treated with **1** and **2**, respectively, by using a 3:1 binding site/signalling subunit molar ratio. This second grafting was accomplished in acetonitrile heated at reflux for 24 h. Thermogravimetric and elemental analyses were carried out in order to determine the amount of binding site grafted onto the surface of the **NA-Pt$_3$** and **NA-Bt$_3$** nanoparticles. Content ratios of 0.0100 and 0.0125 mmol binding site/mmol SiO_2 for butylthiourea- and phenylthiourea-functionalised materials were determined in the prepared solids, respectively. The final molar ratio between binding site and signalling subunit in **NA-Bt$_3$** amounts to 2.4, whereas in the case of **NA-Pt$_3$** this ratio is 3.0. TEM images show a mean diameter of 20 ± 2 nm for both types of hybrid nanoparticles. These bifunctionalised nanoparticles bear up to 1100 attached molecules (the sum of binding sites and signalling subunits). The average distance between two subunits is 12.8 and 11.7 Å for **NA-Bt$_3$** and **NA-Pt$_3$**, respectively.

In order to study the effect exerted by the grafting procedure on the properties of the hybrid materials, a second approach based on the simultaneous grafting of the binding and signalling subunit has been used. Thus, coated nanoparticles characterised by different binding site/signalling subunit ratios were prepared by using compounds **1** and **2** and anthracene derivative **3** simply by modulation of the concentration of the alkoxysilane derivatives in the reaction mixture. With this experimental procedure four coated nanoparticles were prepared. When the molar ratio was set to 1, the coated **NA$_1$Pt$_1$** and **NA$_1$Bt$_1$** nanoparticles were obtained. The composition of the coating for these nanoparticles, bearing in mind the thermogravimetric data and TEM microanalyses, was always found to be close to that of the reaction mixtures. The mol anthracene/mol SiO_2 and mol thiourea/mol SiO_2 ratios in **NA$_1$Pt$_1$** were both 0.0086, whereas for the **NA$_1$Bt$_1$** nanoparticles these ratios were both 0.0130 (see Table 1). The differing amount of anchored groups in the two solids can be attributed to the bulkiness of the butyl subunit when compared with the phenyl one. The average distance between two molecules in **NA$_1$Pt$_1$** amounts to 11.6 Å, whereas the distance between two subunits in **NA$_1$Bt$_1$** is 9.4 Å. This clearly indicates the formation of a more dense monolayer on the nanoparticle surface with butylthiourea binding sites. Again, TEM measurements were carried out in order to determine the mean diameter of the bifunctionalised nanoparticles. From these measurements both **NA$_1$Pt$_1$** and **NA$_1$Bt$_1$** nanoparticles presented nearly the same mean diameter (20 nm). Figure 2 shows an image of both hybrid nanoparticles.

The coated **NA$_1$Pt$_3$** and **NA$_1$Bt$_3$** nanoparticles were prepared by the same grafting procedure described above but changing the molar fraction of the components. In these materials the molar ratio of binding site/signalling subunit was fixed to 3:1. The composition of the coating for these nanoparticles, bearing in mind the thermogravimetric analysis and TEM microanalyses, was found to be relatively close to that present in the reaction mixtures. Also, TEM measurements were carried out in order to determine the

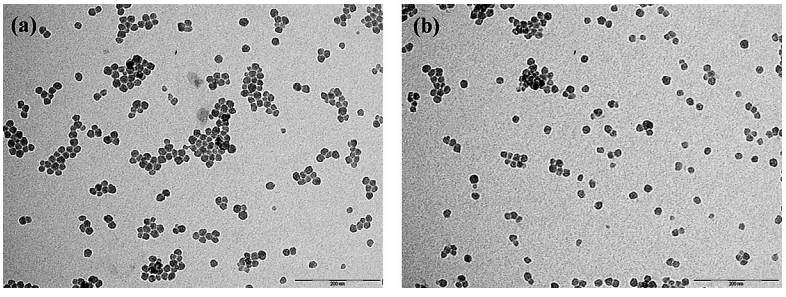

Figure 2. TEM images of hybrid nanoparticles **NA$_1$Bt$_1$** (a) and **NA$_1$Pt$_1$** (b). In both images the bars correspond to 200 nm.

mean diameter of the bifunctionalised nanoparticles. TEM images showed mean diameters of 20 nm for both $\mathbf{NA_1Bt_3}$ and $\mathbf{NA_1Pt_3}$ solids.

As a conclusion, both grafting procedures lead to the preparation of hybrid bifunctionalised silica nanoparticles with well-defined binding site and signalling subunit contents. We think that one advantage of the second approach lies in the fact that only one step of functionalisation is required, which ensures faster synthetic procedures when compared with the sequential grafting of the two subunits. Also, the homogeneity of the monolayer formed with the capped ligands was higher when a one-step grafting procedure was used instead of the consecutive grafting procedure.

Emission Behaviour

This family of coated nanoparticles bearing anthracene as fluorescent signalling subunits and thiourea groups as binding sites are prospective sensory hybrid materials that have the potential ability to recognise anions through changes in fluorescence. The underlying idea was that coordination of certain anions with the thiourea subunit, for instance through hydrogen-bonding interactions, might induce some changes in the emission properties of the anthracene unit by energy- or electron-transfer processes from the anion to the excited anthracene fluorophore.[23,24] As we have cited in the introduction, and as far as we know, only one example dealing with the use of hybrid materials based on silica nanoparticles for anion sensing has been described.

In order to check the ability of the prepared hybrid materials for the selective recognition of anionic species UV/Vis measurements were carried out. Acetonitrile suspensions of **NA** nanoparticles (5 mg in 20 mL) showed the typical anthracene bands centred at ca. 350, 370 and 390 nm. This indicates that the grafting procedure used for the preparation of the bifunctionalised nanoparticles did not fundamentally change the photochemical features of the anthracene moiety. The same UV/Vis features were observed in acetonitrile suspensions (5 mg of nanoparticles in 20 mL of dry acetonitrile) of $\mathbf{NA\text{-}Bt_3}$, $\mathbf{NA\text{-}Pt_3}$, $\mathbf{NA_1Bt_1}$, $\mathbf{NA_1Pt_1}$, $\mathbf{NA_1Bt_3}$ and $\mathbf{NA_1Pt_3}$ that showed in all cases the characteristic bands of the anthracene groups.

The fluorescence of the acetonitrile suspensions of **NA** nanoparticles was measured. Upon excitation at 365 nm, the typical broad emission band with fine structure in the 390–450 nm range was observed. The emission spectrum was also characterised by the absence of emission bands in the 450–600 nm range typical of excimer/exciplex formation. This absence of redshifted bands indicates that there are no interactions between two closely located anthracene subunits (the distance between two anthracene moieties is ca. 22.1 Å). When taking into account the necessary distance for excimer formation in solution, estimated to be ca. 8 Å (in chloroform),[25] the absence of this band in solid **NA** seems to be logical. Again the same emission bands and the absence of redshifted bands were found in acetonitrile suspensions (5 mg in 20 mL) for the bifunctionalised hybrid $\mathbf{NA\text{-}Bt_3}$, $\mathbf{NA\text{-}Pt_3}$, $\mathbf{NA_1Bt_1}$, $\mathbf{NA_1Pt_1}$, $\mathbf{NA_1Bt_3}$ and $\mathbf{NA_1Pt_3}$ nanoparticles. Figure 3 shows the emission spectrum for the $\mathbf{NA\text{-}Pt_3}$ nanoparticles in acetonitrile (λ_{exc} = 365 nm).

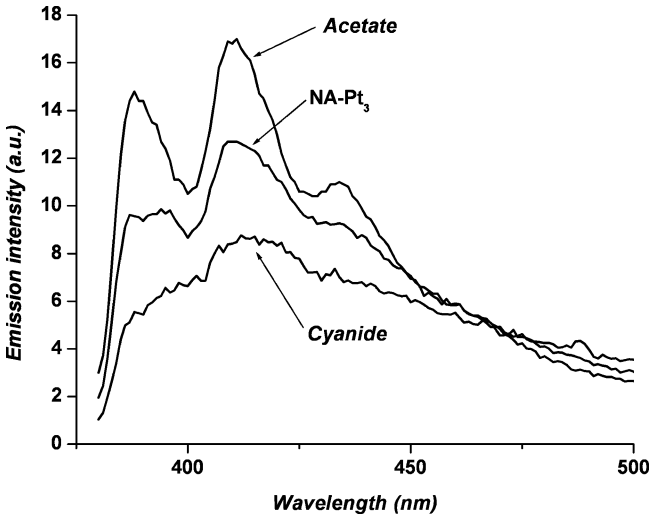

Figure 3. Fluorescence spectra of $\mathbf{NA\text{-}Pt_3}$ hybrid nanoparticles suspended in acetonitrile (λ_{exc} = 365 nm) alone and in the presence of cyanide or acetate.

In order to check the response towards certain organic (acetate, benzoate) and inorganic anions (fluoride, chloride, bromide, cyanide, dihydrogen phosphate and hydrogen sulfate) a series of fluorescence measurements were carried out. Suspensions of the corresponding coated nanoparticles (5 mg) in dry acetonitrile (20 mL) were prepared, and then fluorimetric titrations with the corresponding anions were carried out. The first material tested was **NA**. This solid does not contain binding sites and is a suitable model. The addition of increasing quantities of the target anions to acetonitrile suspension of **NA** induced negligible changes in the intensity of the anthracene emission bands (data not shown). The negative response observed was a clear consequence of the absence of any binding site on the surface of the **NA** nanoparticles.

In a second step we proceeded to study the emission behaviour of the bifunctionalised nanoparticles. The general trends in the emission intensity observed upon addition of target anions could be summarised by the detailed study of the behaviour of acetonitrile suspensions of $\mathbf{NA\text{-}Pt_3}$ nanoparticles. Therefore, fluorescent titrations upon addition of anions to acetonitrile suspensions (5 mg in 20 mL of dry acetonitrile) of $\mathbf{NA\text{-}Pt_3}$ were carried out. As a representative example Figure 4 shows the relative emission changes as the difference between the emission intensity of the $\mathbf{NA\text{-}Pt_3}$ nanoparticles (5 mg in 20 mL) in the presence of 7 equiv. of the corresponding anion (E) and the nanoparticles alone (E_0), in acetonitrile. Three main behaviours were observed (see Figure 4): (i) poor change, (ii) fluorescence enhancement and (iii) fluorescence enhancement coupled with quenching upon reaching a certain quantity of anion equivalents. Thus, the addition of increasing quantities of sulfate

anions did not induce substantial changes in either the intensity or the position of the emission bands. On the other hand, the addition of increasing quantities of phosphate, acetate, benzoate, chloride and bromide anions induced a moderate increase (about 1.4-fold) in the anthracene emission intensity. We attributed this enhancement to coordination of the cited anions with the phenylthiourea binding sites on the surface of the nanoparticles, which resulted in restricting the mobility of the excited anthracene fluorophore and disabling the possibility of de-excitation by non-emissive channels, and thus leading to an increase in the emission intensity. The third behaviour was observed upon addition of cyanide and fluoride anions. In this case, the addition of increasing quantities of both anions (up to 5 equiv.) to acetonitrile suspensions of **NA-Pt$_3$** nanoparticles induced an enhancement in the emission intensity, and then further addition of anion equivalents induced a moderate quenching of the emission intensity (see Figure 4 for the response observed after the addition of 7 equiv. of anions with respect to the total number of binding sites in the nanoparticles). This enhancement/quenching of the emission intensity of the excited anthracene could be explained bearing in mind the fact that cyanide and fluoride are the most basic of all the anions tested. Again, the first emission enhancement could be assigned to a certain restriction in the mobility of the excited anthracene fluorophore upon anion binding, whereas the addition of more equivalents of the cited basic anions would deprotonate the N–H moiety attached directly to the phenyl ring. This proton-transfer reaction would create a negative charge on the binding site that would be responsible for the quenching of the emission intensity through a PET process. These coordination/deprotonation processes of urea and/or thiourea binding sites are well known and, when coupled with dyes or fluorescent units, have been extensively employed for the optical sensing of basic anions in organic solvents.[26] Figure 3 shows the emission spectrum for **NA-Pt$_3$** nanoparticles in acetonitrile (λ_{exc} = 365 nm) in the presence of acetate and sulfate. However, the moderate changes in the emission intensity observed are indicative of weak perturbations of the electronic states of the anthracene fluorophore. These changes are a direct consequence of the weak interactions present between the surface-grafted thiourea binding sites and the target anions.

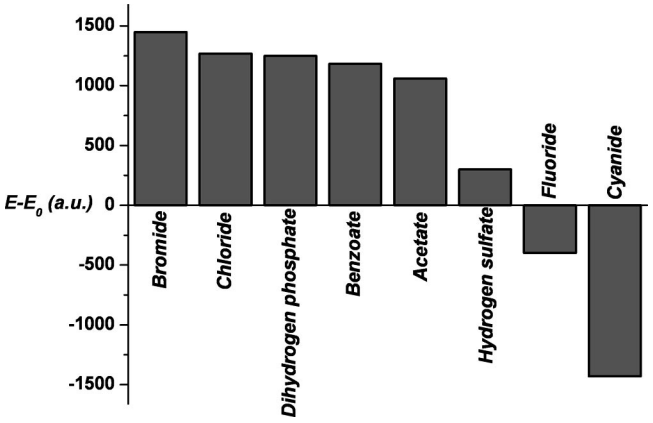

Figure 4. Relative emission changes, as the difference between the emission intensity of the **NA-Pt$_3$** nanoparticles (5 mg in 20 mL) in the presence of 7 equiv. of the corresponding anion (E) and the nanoparticles alone (E_0), in acetonitrile (mol-equiv. with respect to number of binding sites).

In order to complete the characterisation of the interaction of the nanoparticles with anions, the apparent binding constants (adsorption constants) for the interaction of **NA-Pt$_3$** with anions in acetonitrile were determined by performing a Langmuir-type analysis of fluorescence titration data using Equation (1).

$$I = I_L \frac{Kc}{1+Kc} \quad ; \quad c = \frac{-\left\{\frac{1}{K}+\frac{n_M}{V}-c_0\right\}+\sqrt{\left(\frac{1}{K}+\frac{n_M}{V}-c_0\right)^2+\frac{4c_0}{K}}}{2} \qquad (1)$$

Here, K is an adsorption constant that accounts for the interaction between the corresponding anion and the recognition centres anchored to the solid, and I and I_L are the observed intensities at a specific anion concentration and in the presence of an excess of anion (the limiting value), respectively. Additionally, c_0 is the total added salt (in mol L^{-1}), and n_M is the maximum amount of anion (in mol) that could be adsorbed in the monolayer. Finally, V is the volume (in L) in which the experiment was carried out. The formalism that leads to the deduction of Equation (1) is given in the Experimental Section. This equation can be easily applied to the study of the interaction of certain guests with functionalised nanoparticles or other functionalised solid supports.

By using this equation and the experimental titration data, adsorption constants for the acetate, Cl^-, Br^-, benzoate, $H_2PO_4^-$ and HSO_4^- anions have been calculated and are shown in Table 2. Figure 5 shows the emission intensity of solid **NA-Pt$_3$** in the presence of increasing amounts of acetate and HSO_4^- in acetonitrile and the fitting of the experimental data with Equation (1). As can be seen in Table 2, the interaction of the anions with the nanoparticles results in adsorption constants that range from the value observed for acetate (K = 2340) to that found for HSO_4^- (K = 178). The effect of the binding site is reflected in the stability constant found for acetate. In fact, this anion forms the more stable thermodynamic interaction with the nanoparticles and displays the largest adsorption constant. This was expected bearing in mind the structural design of the thiourea moiety, which improves carboxylate binding through the formation of Y-shaped complexes. Additionally, whereas log K for acetate is 3.37, this value is one order of magnitude lower for benzoate (log K = 2.49). This difference was due to the larger size of the benzoate anion, when compared with acetate, which imposes some steric hindrance to the coordination with the thiourea moiety. The constant observed for acetate is quite high. However, this constant is lower than that reported for the interaction of ATP with MCM41-type solids containing anthracene as signalling units.[27]

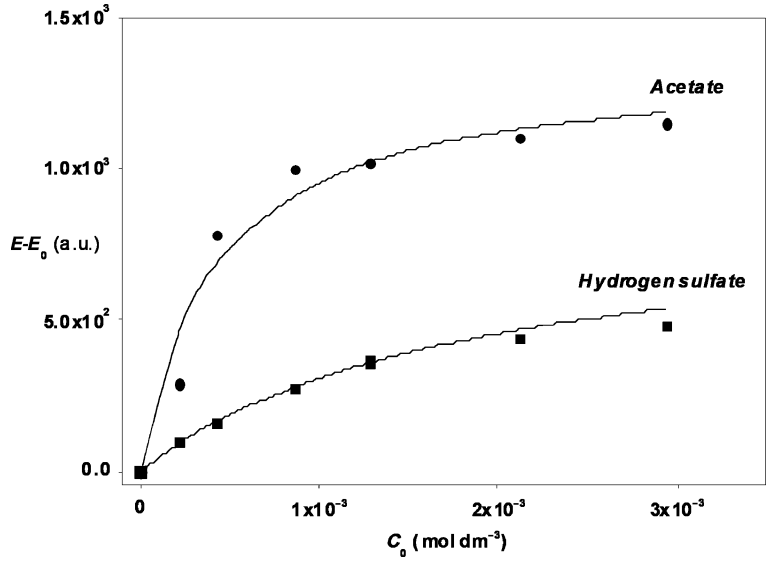

Figure 5. Changes in the emission intensity (λ_{em} = 411 nm) of the anthracene unit of the **NA-Pt$_3$** nanoparticles in the presence of increasing amounts of acetate and hydrogensulfate. The emission intensity has been normalised to 1. The solid line shows the fit obtained with Equation (1).

Table 2. log *K* values obtained for the interaction of **NA-Pt$_3$** nanoparticles with the anions in acetonitrile.

	log *K*[a]
Acetate	3.37
Cl^-	2.91
Br^-	2.27
Benzoate	2.27
$H_2PO_4^-$	2.47
HSO_4^-	2.25

[a] log *K* values have been calculated by using titration curves and Equation (1).

Conclusions

Silica nanoparticles have been treated with the alkoxysilane derivatives *N*-butyl-*N*′-[3-(trimethoxysilyl)propyl]-thiourea (**1**), *N*-phenyl-*N*′-[3-(trimethoxysilyl)propyl]thiourea (**2**) and 3-[(anthracen-10-yl)methylthio]propyltriethoxysilane (**3**) in order to prepare nanoparticles functionalised with both thiourea and anthracene subunits. The functionalisation process was carried out by two different procedures through (i) consecutive or (ii) simultaneous grafting of both subunits. Fluorescence studies on the hybrid nanoparticles were carried out. Typical anthracene absorption and emission bands were observed. The addition of target anions to suspensions of the hybrid nanoparticles in acetonitrile induced moderate changes in the emission intensity with modest patterns of selectivity. The apparent binding constants (adsorption constants) for the interaction of **NA-Pt$_3$** with anions in acetonitrile were determined by performing a Langmuir-type analysis of fluorescence titration data. Despite these results, this procedure is highly modular because it allows the functionalisation of the surface with several binding sites and signalling subunits by routes with a relatively low synthetic effort. We are currently developing novel protocols using nanoparticles for the development of new chromofluorogenic chemosensors for anions.

Experimental Section

General Remarks: Phenyl isothiocyanate, butyl isothiocyanate, (3-aminopropyl)trimethoxysilane, (3-mercaptopropyl)triethoxysilane, 9-(chloromethyl)anthracene and the 30% suspension of LUDOX silica nanoparticles AS-30 Colloidal Silica were purchased from Sigma–Aldrich and were used without any further purification. The solvents were absolute grade and were purchased form Scharlab. The anions were used as tetrabutylammonium salts and were purchased from Aldrich (Cl^-, Br^-, AcO^-, BzO^-, CN^-, HSO_4^- and $H_2PO_4^-$) and Fluka (F^-).

Physical Measurements and Instrumentation: ^1H and ^{13}C NMR spectra were recorded with a Varian Gemini 300 MHz NMR spectrometer. Chemical shifts are reported relative to residual $CHCl_3$. Multiplicities are given as usual. Thermogravimetric analyses were carried out with a Mettler Toledo TGA/SDTA 851^e. Transmission Electron Microscopy (TEM) images of the particles were obtained with a Philips CM10 operating at 20 keV. Samples for TEM were prepared by spreading a drop of nanoparticle solution in HEPES onto standard carbon-coated copper grids (200 mesh). SEM microanalyses were obtained with a JEOL 6300 with a detector WDS of Oxford Instruments. UV/Vis absorption measurements were measured with a Perkin–Elmer Lambda-35 spectrometer. The fluorescence behaviour was studied with an FS900CDT Steady State T-Geometry Fluorimeter from Edinburgh Analytical Instruments. All solutions for photophysical studies were previously degassed. Anion stock solutions for photophysical studies (C = 1×10^{-2} mol dm^{-3}) were prepared in dry acetonitrile.

Synthesis: The syntheses of the alkoxysilane derivatives were carried out according to known procedures. The reaction of (3-aminopropyl)trimethoxysilane with butyl isothiocyanate and phenyl isothiocyanate afforded the trialkoxysilane derivatives **1** and **2** in high yields. Trialkoxysilane derivative **3** was prepared by a nucleo-

philic substitution reaction between (3-mercaptopropyl)triethoxysilane and 9-(chloromethyl)anthracene.

***N*-Butyl-*N*′-[3-(trimethoxysilyl)propyl]thiourea (1):** *N*-butyl-*N*′-[3-(trimethoxysilyl)propyl]thiourea was synthesised by the reaction between (3-aminopropyl)trimethoxysilane (1.75 mL, 10 mmol) and butyl isothiocyanate (1.27 mL, 10 mmol) in CH_2Cl_2 (10 mL) with a few drops of triethylamine (see Scheme 1). After 24 h, the solvent was removed by evaporation, and the product was isolated as a yellowish oil (2.80 g, 95% yield). ^{1}H NMR (300 MHz, $CDCl_3$): δ = 0.60 (t, J = 7.8 Hz, 2 H, -CH_2-Si-), 0.92 (t, J = 6.6 Hz, 3 H, CH_3-CH$_2$-CH$_2$-), 1.35 (m, 2 H, CH$_3$-CH_2-CH$_2$-), 1.55 (m, 2 H, CH$_3$-CH$_2$-CH_2-), 1.61 (t, J = 7.8 Hz, 2 H, -CH_2-CH$_2$-Si-), 3.38 (m, 4 H, -NH-CH_2-CH$_2$-), 3.50 (s, 9 H, CH_3-O-), 6.20 (s, 1 H, -CS-NH-CH$_2$-), 6.37 (s, 1 H, -CH$_2$-NH-CS-) ppm. ^{13}C{^{1}H} NMR (75 MHz, $CDCl_3$): δ = 6.5 (-CH$_2$-Si-), 14.0 (CH$_3$-CH$_2$-CH$_2$-), 20.3 (CH$_3$-CH$_2$-CH$_2$-), 22.5 (-CH$_2$-CH$_2$-Si-), 31.4 (CH$_3$-CH$_2$-CH$_2$-), 47.6 (-NH-CH$_2$-CH$_2$-), 50.8 (CH$_3$-O-), 181 (-NH-CS-NH-) ppm. $C_{11}H_{26}N_2O_3SSi$ (294.49): calcd. C 44.86, H 8.90, N 9.51, S 10.89; found C 44.78, H 8.92, N 9.45, S 10.71.

***N*-Phenyl-*N*′-[3-(trimethoxysilyl)propyl]thiourea (2):** *N*-phenyl-*N*′-[3-(trimethoxysilyl)propyl]thiourea was synthesised by the reaction between (3-aminopropyl)trimethoxysilane (4.77 mL, 27 mmol) and phenyl isothiocyanate (3.27 mL, 27 mmol) in CH_2Cl_2 (10 mL) with a few drops of triethylamine (see Scheme 1). After 24 h, the solvent was removed by evaporation, and the product was isolated as a yellowish oil (6.00 g, 95% yield). ^{1}H NMR (300 MHz, $CDCl_3$): δ = 0.55 (t, J = 7.1 Hz, 2 H, -CH_2-Si-), 1.60 (t, J = 7.1 Hz, 2 H, -CH_2-CH$_2$-Si-), 3.47 (s, 9 H, CH_3-O-), 3.60 (t, J = 7.1 Hz, 2 H, -NH-CH_2-CH$_2$-), 6.27 (s, 1 H, -CS-NH-CH$_2$-), 7.20–7.27 (m, 5 H, C$_6H_5$-NH-), 8.41 (s, 1 H, C$_6$H$_5$-NH-CS-) ppm. ^{13}C{^{1}H} NMR (75 MHz, $CDCl_3$): δ = 6.5 (-CH$_2$-Si-), 22.4 (-CH$_2$-CH$_2$-Si-), 47.6 (-NH-CH$_2$-CH$_2$-), 50.8 (CH$_3$-O-), 125.4 (C_6H$_5$-NH-), 127.2 (C_6H$_5$-NH-), 130.3 (C_6H$_5$-NH-), 136.0 (C_6H$_5$-NH-), 180.7 (-NH-CS-NH-) ppm. $C_{13}H_{22}N_2O_3SSi$ (314.47): calcd. C 49.65, H 7.05, N 8.91, S 10.20; found C 49.72, H 7.15, N 8.78, S 9.96.

3-[(Anthracen-10-yl)methylthio]propyltriethoxysilane (3): 9-(Chloromethyl)anthracene (1.0 g, 4.4 mmol) and (3-mercaptopropyl)triethoxysilane (1.06 mL, 4.4 mmol) were dissolved in dry acetonitrile (50 mL). Potassium carbonate (1.8 g, 13 mmol) was then added, and the mixture was heated at reflux for 24 h. The crude mixture was filtered off in order to remove the excess of potassium carbonate, and the acetonitrile was evaporated to give **3** as a yellowish oil (1.73 g, 95% yield). ^{1}H NMR (300 MHz, $CDCl_3$): δ = 0.78 (t, J = 7.8 Hz, 2 H, -CH_2-Si-), 1.20 (t, J = 7.1 Hz, 9 H, CH_3-CH$_2$-O-), 1.84 (t, J = 7.8 Hz, 2 H, -CH_2-CH$_2$-Si-), 2.70 (t, J = 7.8 Hz, 2 H, -S-CH_2-CH$_2$-CH$_2$-Si), 3.81 (q, J = 7.1 Hz, 6 H, CH$_3$-CH_2-O-), 4.73 (s, 2 H, -S-CH_2-Ar), 7.45 (t, J = 6.5 Hz, 2 H, Ar), 7.55 (t, J = 6.5 Hz, 2 H, Ar), 8.0 (d, J = 6.7 Hz, 2 H, Ar), 8.33 (d, J = 6.7 Hz, 2 H, Ar), 8.40 (s, 1 H, Ar) ppm. ^{13}C{^{1}H} NMR (75 MHz, $CDCl_3$): δ = 8.0 (-CH_2-Si-), 18.3 (CH_3-CH$_2$-O-), 23.3 (-CH_2-CH$_2$-Si-), 35.2 (-S-CH_2-CH$_2$-CH$_2$-Si), 38.3 (-S-CH_2-Ar), 53.3 (CH$_3$-CH_2-O-), 124.1 (Ar), 124.8 (Ar), 126.0 (Ar), 127.0 (Ar), 129.1 (Ar), 130.2 (Ar), 131.5 (Ar), 131.8 (Ar) ppm. $C_{24}H_{32}O_3SSi$ (428.66): calcd. C 67.25, H 7.52, S 7.48; found C 67.37, H 7.60, S 7.34.

Synthesis of Functionalised Silica Nanoparticles: The functionalisation of silica nanoparticles with the signalling subunit and the binding site was carried out according to two distinct approaches. The first approach was based on the consecutive grafting of the two subunits. In the first step nanoparticles functionalised with anthracene moieties were prepared (**NA**), and then the corresponding binding sites (3-fold molar excess based on the content in anthracene) were incorporated onto the nanoparticle surface (**NA-Bt$_3$**, **NA-Pt$_3$**; the dash in this nomenclature indicates the two-step grafting process). The second approach deals with the functionalisation of nanoparticles by the grafting of both subunits (in different molar ratios) in only one synthetic step. These nanoparticles were designated by **NA$_x$Bt$_y$** and **NA$_x$Pt$_y$**, where the absence of the dash between the signalling and binding subunits indicates the simultaneous grafting process, and the values of x and y indicate the molar ratios between the signalling and binding subunits.

Nanoparticles Functionalised with Anthracene (NA): Compound **3** (0.32 g, 0.75 mmol) was placed in a round-bottomed flask and then dissolved with ethanol (100 mL), water (50 mL) and acetic acid (50 mL). Then a water suspension of silica nanoparticles (12 mL LUDOX AS-30 colloidal silica) was added. The reaction mixture was warmed at 80 °C while being stirred for 48 h. After this time, the ethanol was evaporated under reduced pressure, and solid $NaHCO_3$ was added to the suspension until a pH value between 5 and 6 was reached. The silica nanoparticles were isolated by centrifugation and washed with water and acetone. The solid was dried at 70 °C for 16 h.

Nanoparticles Functionalised with Butylthiourea and Anthracene (NA-Bt$_3$): NA nanoparticles (0.75 g) and **1** (0.12 g, 0.7 mmol) were added to dry acetonitrile (50 mL). The resulting mixture was heated at reflux for 24 h. The solid nanoparticles were obtained by centrifugation and were washed several times with water and acetone. The final solid was dried at 70 °C for 16 h.

Nanoparticles Functionalised with Phenylthiourea and Anthracene (NA-Pt$_3$): NA nanoparticles (0.75 g) and **2** (0.12 g, 0.4 mmol) were added to dry acetonitrile (50 mL). The resulting mixture was heated at reflux for 24 h. The solid nanoparticles were obtained by centrifugation and were washed several times with water and acetone. The final solid was dried at 70 °C for 16 h.

Nanoparticles Functionalised with Butylthiourea and Anthracene (NA$_1$Bt$_1$): A colloidal dispersion of LUDOX AS-30 silica nanoparticles (5 mL) was added to a solution containing ethanol (40 mL), water (20 mL) and acetic acid (20 mL). Then compounds **1** (0.084 mmol) and **3** (0.084 mmol) dissolved in dry acetonitrile (5 mL) were added to the nanoparticle suspension, and the resulting mixture was heated at reflux for 48 h. Then the ethanol was removed in a rotary evaporator, and the pH of the water suspension was lowered to 5 by the addition of sodium hydrogencarbonate. The functionalised **NA$_1$Bt$_1$** nanoparticles were isolated by centrifugation at 10000 r.p.m., washed with water and acetone and dried at 70 °C overnight.

Nanoparticles Functionalised with Phenylthiourea and Anthracene (NA$_1$Pt$_1$): A colloidal dispersion of LUDOX AS-30 silica nanoparticles (5 mL) was added to a solution containing ethanol (40 mL), water (20 mL) and acetic acid (20 mL). Then compounds **2** (0.084 mmol) and **3** (0.084 mmol) dissolved in dry acetonitrile (5 mL) were added to the nanoparticle suspension, and the resulting mixture was heated at reflux for 48 h. Then the ethanol was removed in a rotary evaporator, and the pH of the water suspension was lowered to 5 by the addition of sodium hydrogencarbonate. The functionalised **NA$_1$Pt$_1$** nanoparticles were isolated by centrifugation at 10000 r.p.m., washed with water and acetone and dried at 70 °C overnight.

Nanoparticles Functionalised with Butylthiourea and Anthracene (NA$_1$Bt$_3$): A colloidal dispersion of LUDOX AS-30 silica nanoparticles (5 mL) was added to a solution containing ethanol (40 mL), water (20 mL) and acetic acid (20 mL). Then compounds **1** (0.084 mmol) and **3** (0.028 mmol) dissolved in dry acetonitrile (5 mL) were added to the nanoparticle suspension, and the mixture

was heated at reflux for 48 h. Then the ethanol was removed in a rotary evaporator, and the pH of the water suspension was lowered to 5 by the addition of sodium hydrogencarbonate. The functionalised $\mathbf{NA_1Bt_3}$ nanoparticles were isolated by centrifugation at 10000 r.p.m., washed with water and acetone and dried at 70 °C overnight.

Nanoparticles Functionalised with Phenylthiourea and Anthracene ($\mathbf{NA_1Pt_3}$): A colloidal dispersion of LUDOX AS-30 silica nanoparticles (5 mL) was added to a solution containing ethanol (40 mL), water (20 mL) and acetic acid (20 mL). Then compounds **2** (0.084 mmol) and **3** (0.028 mmol) dissolved in dry acetonitrile (5 mL) were added to the nanoparticle suspension, and the resulting mixture was heated at reflux for 48 h. Then the ethanol was removed in a rotary evaporator, and the pH of the water suspension was lowered to 5 by the addition of sodium hydrogencarbonate. The functionalised $\mathbf{NA_1Pt_3}$ nanoparticles were isolated by centrifugation at 10000 r.p.m., washed with water and acetone and dried at 70 °C overnight.

Deduction of Equation (1): The affinity of the solid $\mathbf{NA\text{-}Pt_3}$ nanoparticles for different anions has been studied by using as starting model the well-known Langmuir isotherm for adsorption processes on surfaces. In the Langmuir isotherm the coverage θ is a function of both the temperature and the adsorbate concentration. If the temperature is constant, the coverage is only a function of the concentration and follows Equation (2)

$$\theta = \frac{n_A}{n_M} = \frac{I}{I_L} = \frac{Kc}{1+Kc} \tag{2}$$

where θ is the fraction of adsorbed anion (n_A, in mol) vs. the maximum amount of anion (n_M, in mol) that could be adsorbed in the monolayer. This is equivalent to the ratio between the measured fluorescence intensity at a certain concentration (I) and the fluorescence signal obtained upon saturation with the analyte (I_L). Alternatively, θ can be expressed by the Langmuir adsorption constant K and the concentration c (in mol L^{-1}) of the anion in the equilibrium. Thus, after rearrangement [Equation (3)]:

$$n_A = n_M\theta = \frac{n_M Kc}{1+Kc} \tag{3}$$

Additionally, by taking into account that the total number of moles of anions (n_0) is the sum of the number of moles adsorbed on the monolayer (n_A) and the moles of anions remaining in the solution (n), i.e. $n_0 = n + n_A$, Equation (3) is then transformed into Equation (4):

$$n_0 = n + \frac{n_M Kc}{1+Kc} \tag{4}$$

Dividing by the volume (solution volume V in L), we obtain Equation (5)

$$c_0 = c + \frac{\frac{n_M}{V}Kc}{1+Kc} \tag{5}$$

and finally Equations (6) and (7):

$$Kc^2 + (1 + K\frac{n_M}{V} - Kc_0)c - c_0 = 0 \tag{6}$$

$$c = \frac{-\left\{\frac{1}{K} + \frac{n_M}{V} - c_0\right\} + \sqrt{\left(\frac{1}{K} + \frac{n_M}{V} - c_0\right)^2 + \frac{4c_0}{K}}}{2} \tag{7}$$

From Equation (2) we obtain Equation (8)

$$I = I_L\frac{Kc}{1+Kc} \tag{8}$$

and by substitution of Equation (7) into Equation (8), the final Equation (1) used for fitting of the titration curves is obtained.

Acknowledgments

The authors wish to express their gratitude to the Ministerio de Ciencia y Tecnología (projects CTQ2006-15456-C04-01), for financial support. P. C. thanks the Ministerio de Ciencia y Tecnología for a Torres Quevedo contract.

[1] See for instance: a) A. P. de Silva, H. Q. N. Gunaratne, T. Gunnlaugsson, A. J. M. Huxley, C. P. McCoy, J. T. Rademacher, T. E. Rice, *Chem. Rev.* **1997**, *97*, 1515–1566; b) R. Martínez-Máñez, F. Sancenón, *Chem. Rev.* **2003**, *103*, 4419–4476; c) P. D. Beer, P. A. Gale, *Angew. Chem. Int. Ed.* **2001**, *40*, 486–516; d) R. Martínez-Máñez, F. Sancenón, *Coord. Chem. Rev.* **2006**, *250*, 3081–3093; e) B. Valeur, I. Leray, *Coord. Chem. Rev.* **2000**, *205*, 3–40.

[2] See for instance: a) P. D. Beer, *Chem. Commun.* **1996**, 689–696; b) P. D. Beer, *Coord. Chem. Rev.* **2000**, *205*, 131–155; c) M. E. Padilla-Tosta, R. Martínez-Máñez, T. Pardo, J. Soto, M. J. L. Tendero, *Chem. Commun.* **1997**, 887–888; d) J. M. Lloris, R. Martínez-Máñez, M. E. Padilla-Tosta, T. Pardo, J. Soto, P. D. Beer, J. Cadman, D. K. Smith, *J. Chem. Soc., Dalton Trans.* **1999**, 2359–2369; e) M. J. L. Tendero, A. Benito, J. Cano, J. M. Lloris, R. Martínez-Máñez, J. Soto, P. R. Raithby, M. A. Rennie, *J. Chem. Soc., Dalton Trans.* **1995**, 1643–1644.

[3] See for instance: a) F. Zapata, A. Caballero, A. Espinosa, A. Tárraga, P. Molina, *Org. Lett.* **2008**, *10*, 41–44; b) M. Schmittel, H.-W. Lin, *Angew. Chem. Int. Ed.* **2007**, *46*, 893–896; c) F. Otón, A. Espinosa, A. Tárraga, C. Ramírez de Arellano, P. Molina, *Chem. Eur. J.* **2007**, *13*, 5742–5752; d) F. Otón, A. Tárraga, A. Espinosa, M. D. Velasco, P. Molina, *J. Org. Chem.* **2006**, *71*, 4590–4598; e) D. Jiménez, R. Martínez-Máñez, F. Sancenón, J. V. Ros-Lis, J. Soto, A. Benito, E. García-Breijo, *Eur. J. Inorg. Chem.* **2005**, 2393–2403; f) T. Ghosh, B. G. Maiya, M. W. Wong, *J. Phys. Chem. A* **2004**, *108*, 11249–11259; g) F. Sancenón, A. Benito, F. J. Hernández, J. M. Lloris, R. Martínez-Máñez, T. Pardo, J. Soto, *Eur. J. Inorg. Chem.* **2002**, 866–875; h) J. Maynadie, B. Delavaux-Nicot, S. Fery-Forgues, D. Lavabre, R. Mathieu, *Inorg. Chem.* **2002**, *41*, 5002–5004; i) B. Delavaux-Nicot, S. Fery-Forgues, *Eur. J. Inorg. Chem.* **1999**, 1821–1825; j) P. D. Beer, A. R. G. Graydon, A. O. M. Johnson, D. K. Smith, *Inorg. Chem.* **1997**, *36*, 2112.

[4] a) L. Prodi, F. Bolletta, M. Montalti, N. Zaccheroni, *Coord. Chem. Rev.* **2000**, *205*, 59–83; b) A. Ikeda, S. Shinkai, *Chem. Rev.* **1997**, *97*, 1713–1734; c) J. F. Callan, A. P. de Silva, D. C. Magri, *Tetrahedron* **2005**, *61*, 8551–8588.

[5] a) L. Fabbrizzi, M. Lichelli, G. Rabaioli, A. Taglietti, *Coord. Chem. Rev.* **2000**, *205*, 85–108; b) S. L. Wiskur, H. Aït-Haddou, J. J. Lavigne, E. V. Anslyn, *Acc. Chem. Res.* **2001**, *34*, 963–972.
[6] See for example: a) N. A. Rakow, A. Sen, M. C. Janzen, J. B. Ponder, K. S. Suslick, *Angew. Chem. Int. Ed.* **2005**, *44*, 4528–4532; b) P. L. McGrier, K. M. Solntsev, S. Miao, L. M. Tolbert, O. R. Miranda, V. M. Rotello, U. H. F. Bunz, *Chem. Eur. J.* **2008**, *14*, 4503–4510; c) G. Lu, J. E. Grossman, J. B. Lambert, *J. Org. Chem.* **2006**, *71*, 1769–1776; d) M. H. Lim, S. J. Lippard, *Acc. Chem. Res.* **2007**, *40*, 41–51.
[7] a) L. Basabe-Desmonts, D. N. Reinhoudt, M. Crego-Calama, *Chem. Soc. Rev.* **2007**, *36*, 993–1017; b) M. J. W. Ludden, D. N. Reinhoudt, J. Huskens, *Chem. Soc. Rev.* **2006**, *35*, 1122–1134.
[8] A. B. Descalzo, R. Martínez-Máñez, F. Sancenón, K. Hoffmann, K. Rurack, *Angew. Chem. Int. Ed.* **2006**, *45*, 5924–5948.
[9] a) M. Comes, M. D. Marcos, R. Martínez-Máñez, F. Sancenón, J. Soto, L. A. Villaescusa, P. Amorós, D. Beltrán, *Adv. Mater.* **2004**, *16*, 1783–1786; b) C. Coll, R. Martínez-Máñez, M. D. Marcos, F. Sancenón, J. Soto, *Angew. Chem. Int. Ed.* **2007**, *46*, 1675–1678; c) R. Casasús, E. Aznar, M. D. Marcos, R. Martínez-Máñez, F. Sancenón, J. Soto, P. Amorós, *Angew. Chem. Int. Ed.* **2006**, *45*, 6661–6664; d) M. Comes, G. Rodríguez-López, M. D. Marcos, R. Martínez-Máñez, F. Sancenón, J. Soto, L. A. Villaescusa, P. Amorós, D. Beltrán, *Angew. Chem. Int. Ed.* **2005**, *44*, 2918–2922; e) C. Coll, R. Casasús, E. Aznar, M. D. Marcos, R. Martínez-Máñez, F. Sancenón, J. Soto, P. Amorós, *Chem. Commun.* **2007**, 1957–1959.
[10] a) A. Burns, H. Ow, U. Wiesner, *Chem. Soc. Rev.* **2006**, *35*, 1028–1042; b) L. Prodi, *New J. Chem.* **2005**, *29*, 20–31; c) A. P. R. Johnston, B. J. Battersby, G. A. Lawrie, M. Traut, *Chem. Commun.* **2005**, 848–850; d) E. Katz, I. Willner, *Angew. Chem. Int. Ed.* **2004**, *43*, 6042–6108.
[11] M. Arduini, E. Rampazzo, F. Mancin, P. Tecilla, U. Tonellato, *Inorg. Chim. Acta* **2007**, *360*, 721–727.
[12] a) G. Kickelbick, *Angew. Chem. Int. Ed.* **2004**, *43*, 3102–3104; b) G. Schulz-Ekloff, D. Wöhrle, B. van Duffel, R. A. Schoonheydt, *Microporous Mesoporous Mater.* **2002**, *51*, 91–138.
[13] a) M. Montalti, L. Prodi, N. Zaccheroni, A. Zattoni, P. Reschiglian, G. Falini, *Langmuir* **2004**, *20*, 2989–2991; b) M. Montalti, L. Prodi, N. Zaccheroni, *J. Mat. Chem.* **2005**, *15*, 2810–2814.
[14] K. Ariga, A. Vinu, J. P. Hill, T. Mori, *Coord. Chem. Rev.* **2007**, *251*, 2562–2591.
[15] E. Brasola, F. Mancin, E. Rampazzo, P. Tecilla, U. Tonellato, *Chem. Commun.* **2003**, 3026–3027.
[16] E. Rampazzo, E. Brasola, S. Marcuz, F. Mancin, P. Tecilla, U. Tonellato, *J. Mat. Chem.* **2005**, *15*, 2687–2696.
[17] P. Teolato, E. Rampazzo, M. Arduini, F. Mancin, P. Tecilla, U. Tonellato, *Chem. Eur. J.* **2007**, *13*, 2238–2245.
[18] M. Crego-Calama, D. N. Reinhoudt, *Adv. Mater.* **2001**, *13*, 1171–1174.
[19] L. Basabe-Desmonts, J. Beld, R. S. Zimmerman, J. Hernando, P. Mela, M. F. G. Parajó, N. F. van Hulst, A. van den Berg, D. N. Reinhoudt, M. Crego-Calama, *J. Am. Chem. Soc.* **2004**, *126*, 7293–7299.
[20] P. Calero, E. Aznar, J. M. Lloris, M. D. Marcos, R. Martínez-Máñez, J. V. Ros-Lis, J. Soto, F. Sancenón, *Chem. Commun.* **2008**, 1668–1670.
[21] M. Montalti, L. Prodi, N. Zaccheroni, G. Falini, *J. Am. Chem. Soc.* **2002**, *124*, 13540–13546.
[22] By taking into account the number of millimoles of organic moieties per gram of SiO_2 and the value of the specific surface of the nanoparticle scaffolding, the average coverage (β_A in groups per nm^2) of the surface by the corresponding organic moiety in the different nanoparticles prepared were calculated by using Equation (9): $\beta_A = \alpha_A \cdot 10^{-3} \cdot S^{-1} \cdot 10^{-18} \cdot N_A = \alpha_A \cdot S^{-1}\, 602.3$ (9), where α_A is the organic moiety content ($mmol\,g^{-1}$ SiO_2), S is the specific surface ($230\,m^2\,g^{-1}$) of the nanoparticles and N_A is Avogadro's number.
[23] a) G. De Santis, L. Fabbrizzi, M. Licchelli, A. Poggi, A. Taglietti, *Angew. Chem. Int. Ed. Engl.* **1996**, *35*, 202–204; b) L. Fabbrizzi, G. Francese, M. Licchelli, A. Perotti, A. Taglietti, *Chem. Commun.* **1997**, 581–582; c) L. Fabbrizzi, I. Faravelli, *Chem. Commun.* **1998**, 971–972; d) I. Bruseghini, L. Fabbrizzi, M. Licchelli, A. Taglietti, *Chem. Commun.* **2002**, 1348–1349; e) L. Fabbrizzi, M. Licchelli, F. Mancin, M. Pizzeghello, G. Rabaioli, A. Taglietti, P. Tecilla, U. Tonellato, *Chem. Eur. J.* **2002**, *8*, 94–101.
[24] a) T. Gunnlaugsson, A. P. Davis, J. E. O'Brien, M. Glynn, *Org. Lett.* **2002**, *4*, 2449–2452; b) T. Gunnlaugsson, A. P. Davis, G. M. Hussey, J. Tierney, M. Glynn, *Org. Biomol. Chem.* **2004**, *2*, 1856–1863; c) T. Gunnlaugsson, M. Glynn, G. M. Tocci, P. E. Kruger, F. M. Pfeffer, *Coord. Chem. Rev.* **2006**, *250*, 3094–3117; d) S. E. García-Garrido, C. Caltagirone, M. E. Light, P. A. Gale, *Chem. Commun.* **2007**, 1450–1452.
[25] T. Kobayashi, S. Nagakura, M. Szware, *Chem. Phys.* **1979**, *39*, 105.
[26] See for example: a) V. Amendola, D. Esteban-Gómez, L. Fabbrizzi, M. Licchelli, *Acc. Chem. Res.* **2006**, *39*, 343–353; b) S. Camiolo, P. A. Gale, M. B. Hursthouse, M. E. Light, *Org. Biomol. Chem.* **2003**, *1*, 741–744; c) M. Vázquez, L. Fabbrizzi, A. Taglietti, R. M. Pedrido, A. M. González-Noya, M. R. Bermejo, *Angew. Chem. Int. Ed.* **2004**, *43*, 1962–1965; d) M. Boiocchi, L. Del Boca, D. Esteban-Gómez, L. Fabbrizzi, M. Licchelli, E. Monzani, *J. Am. Chem. Soc.* **2004**, *126*, 16507–16514; e) L. S. Evans, P. A. Gale, M. E. Light, R. Quesada, *Chem. Commun.* **2006**, 965–967; f) A. D. P. Ali, P. E. Kruger, T. Gunnlaugsson, *New J. Chem.* **2008**, *32*, 1153–1161.
[27] a) A. B. Descalzo, M. D. Marcos, R. Martínez-Máñez, J. Soto, D. Beltrán, P. Amorós, *J. Mat. Chem.* **2005**, *15*, 2721–2731; b) A. B. Descalzo, K. Rurak, H. Weisshoff, R. Martínez-Máñez, M. D. Marcos, P. Amorós, K. Hoffmann, J. Soto, *J. Am. Chem. Soc.* **2005**, *127*, 184–200; c) A. B. Descalzo, D. Jiménez, M. D. Marcos, R. Martínez-Máñez, J. Soto, J. El Haskouri, C. Guillém, D. Beltrán, P. Amorós, V. Borrachero, *Adv. Mater.* **2002**, *14*, 966–969.

Received: July 22, 2008
Published Online: November 12, 2008

